Regulation of foot and ankle quasi-stiffness during human hopping across a range of frequencies

Sarah E. Kessler [a], Glen A. Lichtwark [a], Lauren K.M. Welte [b], Michael J. Rainbow [b], Luke A. Kelly [a,*]

[a] *School of Human Movement and Nutrition Sciences, The University of Queensland, Brisbane, Queensland, Australia*
[b] *Department of Mechanical and Materials Engineering, Queen's University, Kingston, Ontario, Canada*

A R T I C L E   I N F O

A B S T R A C T

Human legs operate like springs with adjustable stiffness during locomotion, improving movement economy and versatility. The potential for the foot to contribute to this spring-like mechanism has been established. However, due to previous modelling approaches assuming a rigid-foot segment, it is unknown if ankle and foot quasi-stiffness can be actively regulated, quasi-stiffness being a measure of joint deformation under an applied load. In this study, we sought to determine if midfoot quasi-stiffness was increased in a similar manner as the ankle with increasing load demands, and if these changes were mediated by increased activation of the intrinsic foot muscles. We also quantified differences in measures of ankle joint quasi-stiffness attributable to the modelling assumption of a rigid-foot segment versus a multi-segment foot. Twenty-two healthy individuals performed a single-leg hopping task at three frequencies (2.0 Hz, 2.3 Hz, and 2.6 Hz) while measuring lower limb kinematics, kinetics and muscle activation (EMG). Kinetics and kinematics were calculated at the midfoot and using two different ankle models: rigid-foot model (shank-foot) and an anatomical ankle (shank-calcaneus). Midfoot quasi-stiffness increased with hopping-frequency ($p < 0.05$), while contact phase intrinsic foot muscle activation decreased ($p < 0.05$). The assumption of a rigid-foot model overestimated ankle ROM by ~10° and underestimated ankle quasi-stiffness by 45–60%. This study demonstrates that midfoot quasi-stiffness increases with hopping-frequency; however, the mechanism for these changes remains unclear. Furthermore, this study demonstrates the need to assess the ankle and foot independently, using appropriate models, to avoid significant inaccuracies in basic ankle kinematic and kinetic outputs, such as range of motion and joint quasi-stiffness.

© 2020 Elsevier Ltd. All rights reserved.

1. Introduction

Human legs function like springs during locomotion, utilising elastic mechanisms to recycle mechanical energy (Alexander and Bennet-Clark, 1977; Cavagna and Kaneko, 1977). Storing and returning energy in elastic tissues, like tendons, is thought to reduce the energetic cost of transport by reducing the cost associated with active muscles performing mechanical work (Alexander and Bennet-Clark, 1977; Bobbert et al., 1986; Cavagna and Kaneko, 1977). The central nervous system (CNS) has the capacity to regulate elastic energy storage and return by modulating leg-spring stiffness, in response to variations in the mechanical requirements of locomotion (Ferris et al., 1998). Leg-spring stiffness is altered on an individual joint basis with each joint's quasi-stiffness tuned to

resist deformation under load. This actively regulated joint quasi-stiffness allows optimisation of movement patterns that are characterised by continuous alterations in speed and direction (Arampatzis et al., 1999; Farley et al., 1991b; Farley and Gonzalez, 1996; McMahon and Cheng, 1990).

The ankle joint complex is a key contributor to the leg-spring function, with elastic recoil of the Achilles tendon contributing between 16 and 38% of the mechanical energy to the system during ballistic movements (Ker et al., 1987; Lichtwark and Wilson, 2005). The ankle joint plays a key role in our capacity to adjust our leg mechanics, with the CNS modulating ankle joint quasi-stiffness to account for increases in speed (Arampatzis et al., 1999; Farley et al., 1991) and surface compliance (Ferris and Farley, 1997; Ferris et al., 1998; Kerdok et al., 2002). As we run or hop faster, the CNS regulates this quasi-stiffness via fluctuations in activation of antagonist and agonist muscles (Muller et al., 2012) modulating how much the joint deforms under a given load (Latash and Zatsiorsky, 1993). These CNS-controlled adaptations allow for

efficient movement across a variety of locomotor tasks (Ferris and Farley, 1997; McMahon and Cheng, 1990).

Despite the importance of the ankle for leg-spring function, much of our understanding of ankle joint mechanics during human locomotion is based on oversimplified 'rigid' foot models (Blickhan and Full, 1993; Farley and Gonzalez, 1996; McMahon and Cheng, 1990). These studies have modelled the ankle joint as the rotation of a single rigid-foot segment about the leg. This modelling approach assumes that the joints of the midfoot do not rotate or translate as the foot is loaded. The recent implementation of multi-segment foot models (Bruening et al., 2012) highlights that modelling the foot in this way leads to over-estimations of angular excursion and mechanical power at the ankle joint (Zelik and Honert, 2018). Over-estimations of ankle excursion will result in over-estimations of ankle power, while simultaneously underappreciating the power generated by structures within the foot. Such overestimations of ankle plantar flexor power requirements could lead to inaccurate estimates of the activation and energetics of the plantar flexor muscle group (Uchida et al., 2016a; Uchida et al., 2016b) or could potentially result in inappropriate prosthetic designs for generating power at the foot and ankle (Zelik and Honert, 2018). Early cadaveric (Ker et al., 1987) and recent in-vivo (Stearne et al., 2016) studies have further confirmed the importance of the foot in contributing to leg-spring mechanics, suggesting that the foot can contribute between 8 and 17% of the mechanical energy required for a stride. In this way, the human foot also functions like a spring during locomotion, compressing and recoiling during stance phase, in-series with the entire lower limb (Ker et al., 1987; Stearne et al., 2016). The magnitude of deformation and torques generated at the midfoot are likely far greater than previously appreciated.

The spring-like function of the foot is governed by both passive elastic structures and active structures, e.g. plantar intrinsic foot muscles (Kura et al., 1997; Leardini et al., 1999). The intrinsic foot muscles have been shown to activate in response to arch deformation under load (Kelly et al., 2014a; Kelly et al., 2014b), but the mechanical reason remains unclear. It is possible the muscles serve to protect the plantar fascia from excessive strain (Kelly et al., 2014a) or modulate midfoot quasi-stiffness in response to increased postural and loading demands (Kelly et al., 2014a; Kelly et al., 2014b). However, contradictory findings have shown that midfoot quasi-stiffness does not change during running when recruitment of the intrinsic muscles is inhibited via a selective motor-nerve block (Farris et al., 2019). The unchanged midfoot quasi-stiffness in the presence of a nerve block condition could be due to participants utilizing different running strategies to maintain speed, thus obscuring changes to midfoot quasi-stiffness. These seemingly contradictory findings suggest we need further insight into the mechanics of the midfoot using a controlled movement pattern, to understand how the CNS regulates midfoot mechanics.

In this study, we sought to better understand the ability of the midfoot to contribute to leg stiffness during bouncing-gaits. We examined ankle and midfoot mechanics during a single-leg hopping task at different hopping-frequencies. Single-leg hopping is a convenient model for bouncing-gaits as system stiffness can be manipulated while limiting external factors that could obscure changes to midfoot quasi-stiffness. The aim of this study was threefold: 1) determine if midfoot quasi-stiffness is modulated in a manner similar to the ankle 2) determine the role of intrinsic foot muscles in stiffening the midfoot and 3) determine how the assumptions of a rigid-foot model influence interpretation of ankle mechanics. We hypothesized that with increasing hopping-frequency, there would be a concurrent increase in ankle and midfoot quasi-stiffness coupled with an increase in intrinsic foot muscle activation. We further hypothesized that modelling the ankle as a shank and single, rigid-segment foot would result in a significantly less-stiff ankle when compared with the anatomical ankle model.

2. Methods

2.1. Participants

Twenty-two healthy participants volunteered to participate in this study (seven females, fifteen males, weight 73.22 ± 11.57 kg). Participants were excluded if they had a history of lower limb injury in the previous 12 months, or diagnosed neurological or cardiovascular disease. The procedures were approved by the local scientific ethical committee and performed according to the Declaration of Helsinki. The study protocol was approved by both The University of Queensland and Queen's University institutional ethics review boards (IRB numbers; 2018001146, 6022292, respectively). Participants read and completed an ethics approved consent form and questionnaire.

2.2. Experimental task

Prior to data collection, participants were provided time to familiarize themselves with the hopping tasks. Each participant was instructed to practice hopping on their right foot until they felt comfortable. Following the familiarization, each participant completed three single-leg hopping tasks at pre-determined frequencies, 2.0 Hz (slow), 2.3 Hz (intermediate), and 2.6 Hz (fast), performed in a counterbalanced order. Frequencies were selected based on data from Farley et al. which suggests preferred hopping-frequency is approximately 2.2 Hz (Farley et al., 1991a). For each prescribed hopping-frequency, a digital metronome was provided and participants were asked to match the metronome to the best of their ability. When it was visually determined that the participants were in time with the metronome, data collection was manually triggered for a period of 10 s.

2.3. Data collection

2.3.1. Experimental set-up

This experiment was performed across two separate laboratories at Queen's University 'QU' (Canada) and The University of Queensland, 'UQ' (Australia). Data collection was performed across two sites as a part of a larger funded, multi-site project (ARC DP160101117). Experimental procedures and equipment were kept as consistent as possible, only differing in the force plate model, analog sample rate, and ultrasound machine model. At QU, the force plate (AMTI Optima, AMTI, Watertown, MA) was sampled at 1125 Hz, whereas, at UQ (AMTI, OR6-7-1000, Watertown, MA) was sampled between 1250 Hz and 5000 Hz. At QU, the ultrasound machine used for guiding intrinsic fine-wire insertion was 6.25 MHz linear array (Verasonics, Kirkland WA, USA); whereas, UQ used 10 MHz linear array (SonixTouch, Ultrasonix, BC, Canada). Finally, QU collected muscle activity on the soleus (SOL), while UQ recorded tibialis anterior (TA) due to the collection at UQ being part of a larger data collection. Otherwise, all equipment and procedures were identical.

2.3.2. Data acquisition

Sixteen *retro*-reflective markers (6.4 mm, B&L Engineering, Santa Ana, CA) were placed on anatomical landmarks of the foot and ankle in accordance with a previously described multi-segment foot model ((Leardini et al., 2007), Fig. 1a). Additional markers were placed on the medial and lateral malleolus and the medial and lateral femoral epicondyles to define the shank seg-
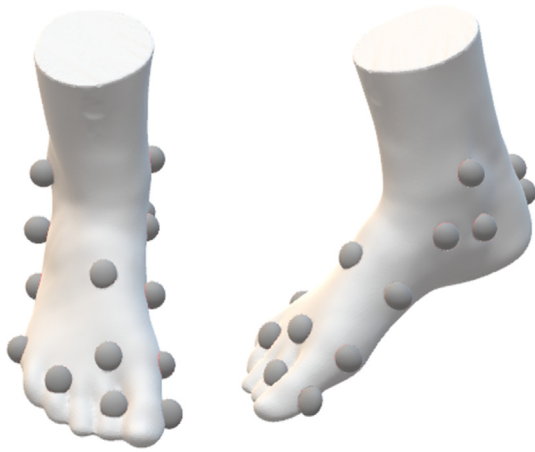
Fig. 1. Foot marker placement for the multi-segment foot model. The markers were placed on the bony landmarks of the feet in accordance with the IOR foot model (Leardini et al., 1999). Using these marker placements, movement of the hindfoot, midfoot, and forefoot can be calculated using a 6 degree of freedom model.

ment. Rigid marker clusters were secured to the lateral aspect of the shank to track its motion throughout the trial. Three-dimensional (3D) marker positions were captured using an optical motion capture system (Qualysis AB, Gothenburg, Sweden), sampled between 125 and 500 Hz.

2.3.3. Muscle activation

Activation of muscles within the arch of the foot were recorded using fine-wire electromyography (EMG). Electrodes were inserted into the abductor hallucis (AH, n = 18) and flexor digitorum brevis (FDB, n = 18) muscles of the right foot under ultrasound guidance (Kelly et al., 2012). Signal quality was assessed by asking participants to flex and extend their toes while observing the EMG signal. If motion artefact or poor signal-to-noise ratio was evident, the electrode positions were slightly adjusted by approximately 1–2mm. Three participants experienced discomfort with the fine-wire EMG, and fine-wire was not recorded for these participants. One participant had poor signal-to-noise ratio, and as such their fine-wire EMG was excluded from the data.

Leg muscle activation data was collected using skin mounted surface electrodes on the right leg using Ag-AgCl electrodes with a 20 mm inter-electrode distance (Tyco Healthcare Group, Neustadt, Germany) from the medial gastrocnemius (GM, n = 22), soleus (SOL, Canada, n = 8), and tibialis anterior (TA, Australia, n = 14). Prior to surface electrode placement, the skin was shaved, abraded and cleaned with isopropyl alcohol. All EMG signals were collected at 4 kHz, amplified 1000 times and recorded with a bandwidth of 30–1000 Hz (MA300, Motion Labs, LA, USA). To reduce the risk of movement artefact, all EMG pre-amplifiers and cabling were secured to the leg using cohesive bandage.

2.4. Data processing

The 3D marker trajectories were digitized and identified in Qualysis Track Manager (Qualysis Track Manager, Gothenburg, Sweden) and exported to Visual 3D (C-Motion, Germantown, MD, USA) for further processing. Marker trajectories were filtered using a 2nd order recursive low-pass Butterworth filter with a cut-off frequency of 10 Hz (Kelly et al., 2018). Ground reaction force data were filtered with a 2nd order recursive low pass Butterworth filter at 30 Hz (Kelly et al., 2016).

2.5. Data analysis

2.5.1. Foot and ankle mechanics

Two different ankle models were created. Consistent with previous studies, a 'traditional' ankle model was created by assuming the foot was a single, rigid-segment that rotated around the shank. An anatomical ankle was also created by tracking the rotation of the calcaneus about the shank. The segment definitions and tracking targets for the rigid-foot and anatomical ankle have been previously described (Leardini et al., 2007). We further computed kinematics of the midfoot (metatarsals-calcaneus) (Leardini et al., 1999) and the metatarsophalangeal (MTP, toes-metatarsals) joints. Joint rotations were calculated in accordance with International Society of Biomechanics recommendations (Wu and Cavanagh, 1995). Range of motion (ROM) for each joint was calculated as the difference of peak extension minus peak flexion.

Impulse, contact time (CT), and jump height were calculated for each hop. Impulse was calculated as the integral of force and time during contact (Domire and Challis, 2007). Jump height was calculated according to equations of uniform acceleration using take-off velocity (Moir, 2008). Take-off velocity was calculated the instant the foot left the ground by differentiating the Z-coordinate of the average pelvis coordinate (centroid of R-PSIS, R-ASIS, L-PSIS, L-ASIS).

An inverse dynamics approach was applied to estimate the internal moments generated about each of the joints in the sagittal plane. Joint quasi-stiffness was calculated for each joint using a previously described method (Farris et al., 2019; Kelly et al., 2014b; Zhou et al., 2015). Briefly, joint quasi-stiffness was calculated by fitting a straight line to the joint moment vs. angle curve, during the negative work (loading) phase and calculating the slope of the line. We examined the negative work phase as quasi-stiffness is defined as the resistance to deformation under load and would therefore only be appropriate to measure during the loading phase.

2.5.2. Muscle activation

Electromyography data was processed in Matlab 2018b (Natick, Massachusetts, USA). The intrinsic EMG was de-trended, then high-pass filtered using a fourth-order Butterworth filter at 40 Hz to remove unwanted low-frequency movement artefact (Kelly et al., 2019; Kelly et al., 2016). Subsequently, a root mean square (RMS) signal was calculated. The surface EMG underwent DC-offset removal, rectification and an RMS. All EMG signals were normalized as a percent of maximum muscle activation (Kelly et al., 2014b; Riddick et al., 2019). Individual maximum muscle activation for all muscles was determined by taking the peak amplitude across all three hopping-frequencies, for each individual muscle.

2.5.3. Data reduction

A single hop cycle was defined from toe-off to the next consecutive toe-off. Toe-off was defined as the instant the vertical ground reaction force (GRFz) signal passed below 50 N, and contact was defined as the instant when GRFz exceeded 50 N. Data was isolated for each individual hop. Individual hops were only included in the analysis if they fell within ± 6% of the expected hopping-duration. The cut-off of 6% was chosen as it provides the largest window of variation (0.03 s to 0.023 s) for each frequency while still preventing overlap of the different frequencies.

Individual means for joint angles, moments, and quasi-stiffness were calculated for each participant by averaging the data across all eligible hops in that condition. Mean EMG activation for the entire hop was divided by time and calculated for each hop cycle. Average muscle activation during flight and contact were also cal-

Table 1

Group Mean ± SD for peak vertical ground reaction force (GRFz), contact time, jump height and impulse across all three hopping frequencies. GRF$_z$ data was normalized to body weight (BW). Contact time represents the average time from contact to toe-off in seconds. Impulse was calculated as the integral of force and contact time. [α]Denotes a significant main effect of hopping-frequency (p < 0.05).

Frequencies	Temporal data			
	Peak GRF$_z^{\alpha}$ (BW)	Contact time[α] (s)	Jump height[α] (cm)	Impulse[α] (N/s)
Slow	2.30 ± 0.04	0.35 ± 0.02	2.02 ± 0.74	104.00 ± 17.61
Medium	2.43 ± 0.04	0.30 ± 0.02	1.70 ± 0.63	94.31 ± 14.54
Fast	2.47 ± 0.04	0.27 ± 0.02	1.44 ± 0.47	86.23 ± 13.19

culated. The GRFz and joint moment data were normalised to bodyweight (BW).

2.6. Statistics

Statistics were calculated using the Statistical Package for Social Sciences (SPSS) program (IBM Corp. Released 2017. IBM SPSS Statistics for Windows, Version 25.0. Armonk, NY: IBM Corp.), A Shapiro-Wilk normality test was used to determine if the data was normally distributed (p < 0.05). All data was normally distributed except for CT, midfoot range of motion (ROM), and TA activation (contact phase).

Multiple one-way repeated-measures ANOVAs were used for all normally distributed data with the repeated factor of 'hopping-frequency' to examine within-subject effects of: midfoot quasi-stiffness, midfoot ROM and midfoot peak moment, as well as, muscle activation (EMG) for each muscle across contact, flight, and whole hop.

Three independent two-way repeated-measures ANOVAs were used to determine differences between ankle modelling approaches (traditional vs. anatomical ankle) and hopping-frequency (2.0 Hz vs 2.3 Hz vs 2.6 Hz) for ROM, peak moment and quasi-stiffness. All comparisons were within-subject with a repeated-measures design. Statistical significance was set at p < 0.05. Effect size (ES) calculations for parametric one-way and two-way ANOVAs are expressed as partial ETA[2] (Tabachnick and Fidell, 2001; Thompson, 2006). *(The specific tests used are outlined further in supplementary table 1.)*

Table 2

Group Mean ± SD kinematic and kinetic data across the three different hopping-frequencies. Range of motion was calculated as the absolute value of the difference between peak plantarflexion and peak dorsiflexion. Peak moments were normalized to body mass (kg) and averaged across all eligible hops. Stiffness was calculated by applying a best fit line to the angle-moment curve during the negative power phase (loading phase) for each joint. Hopping-frequency had a significant effect on peak moment across all three joints, with the slowest frequency producing the lowest moment (p < 0.05). Across the two ankle joint models – there was a significant effect of model type and frequency, with differences compounded by the interaction between the model type and frequency (p < 0.05). (*Ankle:* [α]Denotes an effect of Model, [β]Denotes an effect of hopping-frequency, [Ω]Denotes an interaction Effect, *Midfoot:* [Ψ] Denotes an effect of hopping-frequency).

Rates:	Traditional Ankle	Anatomical Ankle	Midfoot
	Range of Motion (°) [α, β, Ω, Ψ]		
Slow	34.45 ± 5.04	24.52 ± 4.28	14.46 ± 3.19
Medium	30.37 ± 3.88	20.87 ± 3.75	13.72 ± 2.71
Fast	25.56 ± 3.49	16.92 ± 2.99	12.52 ± 2.89
	Moments (Nm·kg^{-1}) [α, β, Ω, Ψ]		
Slow	3.48 ± 0.46	3.45 ± 0.46	1.55 ± 0.35
Medium	3.85 ± 0.44	3.82 ± 0.44	1.71 ± 0.33
Fast	3.93 ± 0.46	3.91 ± 0.46	1.77 ± 0.37
	Stiffness (Nm·kg^{-1}·deg^{-1}) [α, β, Ω, Ψ]		
Slow	0.11 ± 0.02	0.16 ± 0.04	0.12 ± 0.02
Medium	0.14 ± 0.03	0.21 ± 0.05	0.14 ± 0.02
Fast	0.17 ± 0.03	0.28 ± 0.07	0.15 ± 0.02

3. Results

Across all participants, we analysed 70.5% of hops at the slowest hopping-frequency, 89.0% of hops at the intermediate frequency and 87.1% of hops at the fastest frequency. A minimum of 6 hops were reported from each participant at each condition, with two exceptions (at 2.0 Hz: two participants completed 2 and 5 hops, respectively, at the correct frequency).
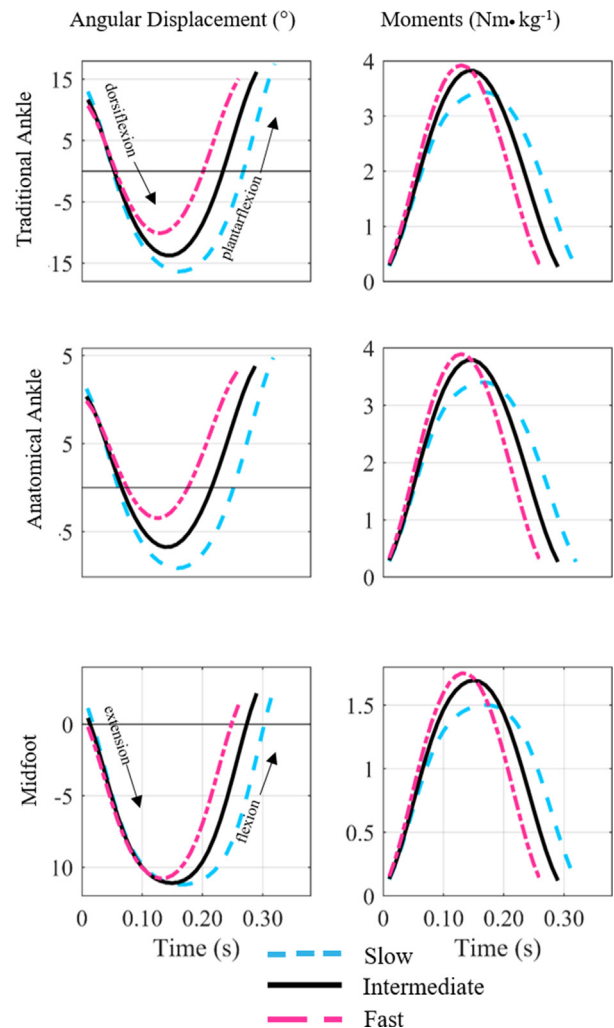

Fig. 2. Group mean data of angular displacement and moments across contact phase for three different frequencies (cyan – 2.0 Hz, black – 2.3 Hz and pink – 2.6 Hz). The traditional ankle (top) is modelled with a rigid-foot segment, while the anatomical ankle (middle) is modelled as the rotation of the calcaneus relative to the shank. The midfoot (bottom) is modelled as rotation of the metatarsals relative to the calcaneus.

3.1. Kinematics and kinetics

Spatial-temporal data is presented in Table 1. There was a significant effect of hopping-frequency on peak GRFz, CT, and impulse (all p < 0.05). Peak GRFz increased and contact time decreased as hopping-frequency increased (Table 1). Impulse also decreased as hopping-frequency increased (104.00 N/s at the slowest frequency to 86.23 N/s at the fastest frequency).

3.2. Ankle mechanics

3.2.1. Effect of Hopping-Frequency
Kinematics for both ankle models are represented in Table 2 and Fig. 2. There was a main effect of hopping-frequency on ankle ROM, peak moment and quasi-stiffness (all p < 0.05). Ankle joint ROM decreased (ES: 0.89) and peak moment increased as hopping-frequency increased (ES: 0.62). Accordingly, ankle joint quasi-stiffness also increased with hopping-frequency (ES: 0.87) (Fig. 3).

3.2.2. Effect of model
There was a global effect of model type on ROM, peak moments and ankle quasi-stiffness (all p < 0.05). When the ankle was modelled with a rigid-foot segment a greater ROM was observed, compared to the anatomical ankle (ES: 0.96). A slightly larger peak moment was reported when the ankle was modelled with a rigid-foot segment (ES: 0.41). However, due to the considerable increase in ROM, ankle joint quasi-stiffness was substantially lower when modelled with the rigid-foot segment, compared to the anatomical ankle (ES: 0.89).

3.2.3. Model*Frequency
There was an interaction effect between ankle model and hopping-frequency for ROM, peak moment, and quasi-stiffness (all p < 0.05). The ROM difference between the model types was greater at slower frequencies (ES: 0.41). The ankle moment difference between models was greatest at the slowest frequency (ES: 0.22) while the difference in quasi-stiffness increased with hopping-frequency (ES: 0.79).

3.3. Midfoot mechanics

Midfoot angles and moments are represented in Fig. 2 and Table 2. As hopping-frequency increased there were significant changes in midfoot ROM, peak moment, and quasi-stiffness (all p < 0.05). With increasing hopping-frequency, ROM decreased while peak moments (ES: 0.58) and quasi-stiffness increased (ES: 0.85) (Fig. 3, Table 2).

3.4. Muscle activation

Average muscle activation is represented in Fig. 4 and Table 3. Across the hop cycle, average muscle activation increased with increasing hopping-frequency for all muscles except FDB (p < 0.05, ES: GM: 0.76, SOL: 0.74, TA: 0.80, AH: 0.69, and FDB: p = 0.07). During contact, there was a significant increase in TA activation (ES: n/a) with significant decreases in GM and FDB activation (ES: 0.55, 0.21, respectively). There was no change in SOL or AH activation during contact (p = 0.24, 0.46, respectively). During flight, there was an increase in activation of GM, SOL and AH (p < 0.05, ES: 0.50, 0.85, 0.34, respectively), with no change to activation during flight for TA or FDB (p = 0.83, 0.20, respectively).

4. Discussion

We sought to elucidate the individual contributions of the midfoot and ankle to lower limb mechanics during single-leg hopping at varying frequencies. As hypothesized, we found that the midfoot behaves in a spring-like manner, coupled closely with the behaviour at the ankle, increasing quasi-stiffness with increasing hopping-frequency. Surprisingly, the increase in both ankle and midfoot quasi-stiffness was not met by an increase in contact phase intrinsic foot muscle activation, but instead by a decrease in activation. Notably, there was an increase in the pre-activation of the GM, SOL, and AH muscles, which may play a key role in stiffening the foot and ankle complex, allowing force to rise rapidly with increasing hopping-frequency. We found that modelling the foot as a rigid-link segment leads to underestimations in ankle
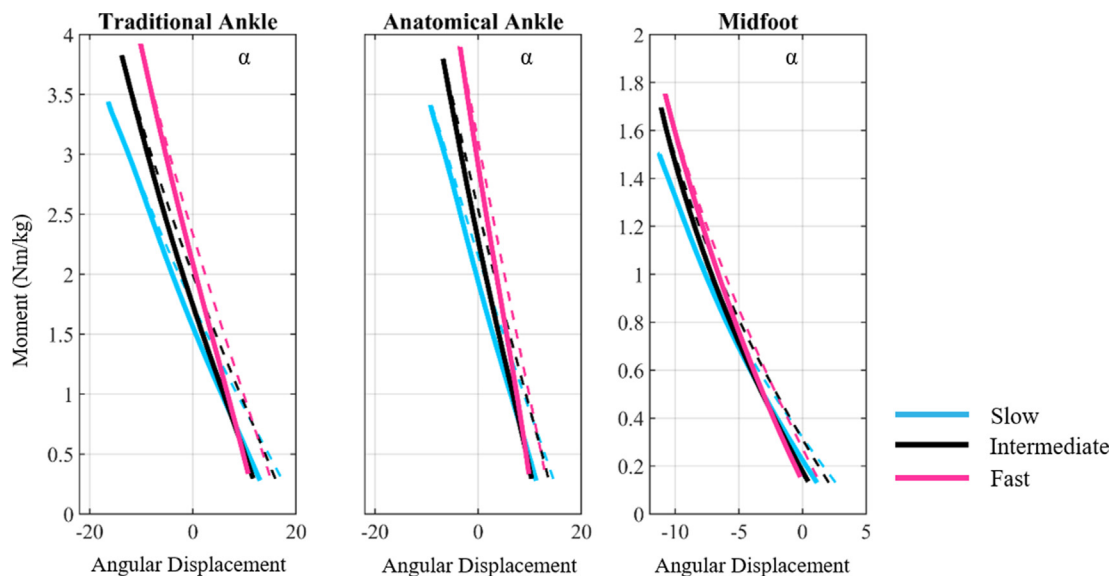

Fig. 3. Quasi-stiffness of the traditional ankle, anatomical ankle, and the midfoot joints across contact phase for three different frequencies (cyan – 2.0 Hz, black – 2.3 Hz and pink – 2.6 Hz). Quasi-stiffness is calculated during the loading phase (solid line) in the sagittal plane with a traditional ankle model (rigid-foot rotating around the shank), anatomical ankle (calcaneus rotating around the shank) and the midfoot (metatarsals rotating around the calcaneus). α -Denotes quasi stiffness significantly increased with hopping-frequency for all joints.
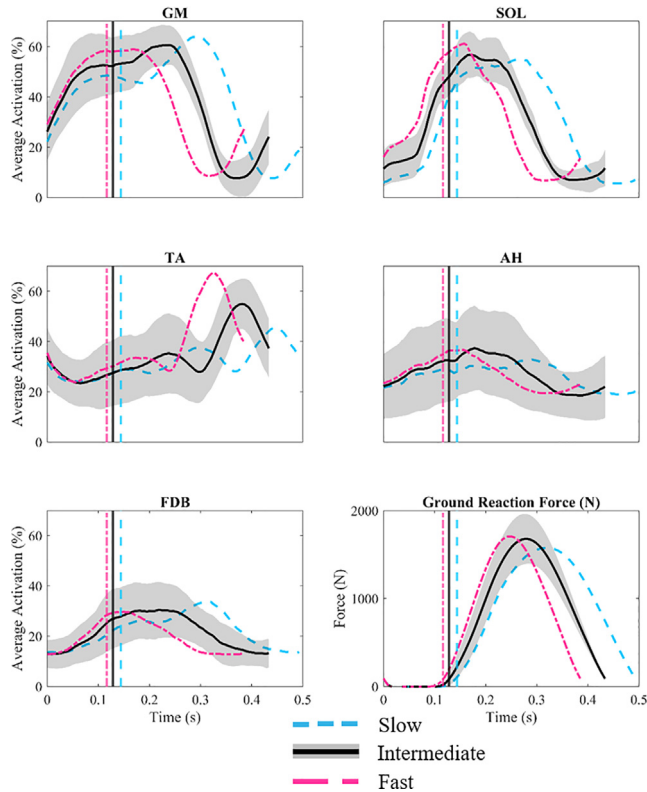
Fig. 4. Group Mean Muscle Activity for the medial gastrocnemius (GM), soleous (SOL), tibialis anterior (TA), abductor hallucis (AH) and flexor digitorum brevis (FDB) during single-leg hopping at three frequencies (cyan − 2.0 Hz, black and grey-2.3 Hz (±1SD) and pink − 2.6 Hz). The bottom-right represents the ground reaction forces for the different frequencies and serves as a guideline for when the hop cycle begins and ends for each frequency. Vertical lines denote foot contact for each condition.

quasi-stiffness and potentially reduces the measurement resolution when quantifying ankle mechanics.

Midfoot quasi-stiffness increased as hopping-frequency increased, in line with changes observed at the ankle. The observed change in quasi-stiffness could potentially be explained via passive (Stearne et al., 2016; Welte et al., 2018; Ker et al., 1987) or active mechanisms (Farris et al., 2019; Kelly et al., 2014, 2018). Passively, the plantar aponeurosis was originally believed to stiffen the foot via the windlass mechanism, whereby extension of the MTP joint winds the aponeurosis around the metatarsal heads shortening, raising, and stiffening the arch (Hicks, 1954). Given that MTP joint kinematics did not vary between hopping-frequencies, it is unlikely the changes in midfoot quasi-stiffness observed here can be attributed to the windlass mechanism.

We hypothesized that intrinsic foot muscle activation would increase with hopping-frequency, contributing to increased midfoot quasi-stiffness. However, we observed the opposite, with intrinsic foot muscle activation decreasing during contact phase. This finding can potentially be explained by the observed reduction in vertical impulse, which suggests that less negative and positive mechanical work was performed at the centre of mass. Therefore, potentially, activation of foot and leg muscles during contact decreased in line with the decreased mechanical work demands (Riddick et al., 2019), despite increased peak joint moments. It is also possible the increase in midfoot and ankle quasi-stiffness could be explained by the increase in pre-activation of the GM, SOL, and AH. The increase in muscle activation prior to foot contact may help to stiffen the muscle tendon unit at low forces, increasing the quasi-stiffness of the joint in preparation for the loading phase of the hop cycle.

Table 3

Group Mean ± SD electromyography (EMG) across the total hopping cycle (Total), Flight, and Contact phases. EMG was normalized to the individual's maximum activation of each muscle, across all three frequencies. Data is averaged over time, resulting in average EMG activation per second. Number of participants represented in each muscle group for all three hopping frequencies: GM (n = 22), SOL (n = 8), TA (n = 14), AH (n = 18), FDB (n = 18).

Frequencies	Medial gastrocnemius[α,β,Ω]			Soleus[α,Ω]			Tibialis anterior[α,β]			Abductor hallucis[α,Ω]			Flexor digitorum brevis[β]		
	Total	Flight	Contact	Total	Flight	Contact	Total	Flight	Contact	Total	Flight	Contact	Total	Flight	Contact
Slow	81.1% (15%)	42.5% (10%)	39.1% (6%)	59.5% (7%)	19.0% (4%)	33.3% (4%)	63.1% (18%)	25.6% (9%)	33.3% (9%)	55.0% (27%)	27.8% (15%)	26.8% (13%)	46.4% (17%)	17.3% (7%)	25.1% (9%)
Medium	93.1% (18%)	46.3% (12%)	37.5% (6%)	70.4% (11%)	24.0% (5%)	31.9% (4%)	76.7% (22%)	25.9% (10%)	36.4% (10%)	65.9% (31%)	29.8% (15%)	27.9% (13%)	50.8% (17%)	17.8% (7%)	23.7% (7%)
Fast	101.2% (19%)	48.8% (11%)	34.8 (6%)	81.0% (6%)	32.5% (2%)	30.6% (4%)	95.3% (28%)	26.4% (11%)	41.3% (11%)	73.8% (34%)	31.9% (17%)	27.0% (12%)	53.0% (20%)	19.2% (8%)	21.0% (8%)

α) Significant difference across the entire duty cycle. β) Significant difference during contact Ω) Significant difference in EMG activation during flight.

Our data demonstrates that the application of a rigid-foot model leads to substantial miscalculations of ankle joint excursion and quasi-stiffness ($45\% - 60\%$). The source of divergence between the two models is seemingly straightforward: the traditional ankle creates a rigid-segment foot, incapable of deforming, whereas, the anatomical ankle allows for deformation of the arch independent of the ankle. It appears, given the interaction effect found here, as force requirements increase, the rigid-foot model becomes more inaccurate potentially leading to overestimations of work and power at the ankle under increasing loads. One consequence of inaccurate power measurements at the ankle is that it overstates the contribution of plantar flexors and particularly the Achilles tendon, which contributes most of the positive power. With an accurate understanding of the plantar flexors, and therefore power generation about the ankle, the current standards of gait retraining therapies (Brehm et al., 2008; Rouhani et al., 2011), prosthesis development (Zelik and Honert, 2018), and surgical interventions could be significantly improved.

This study should be interpreted within the context of a few limitations. We chose to look at hopping due to the controlled nature of the task, however, most bouncing-gaits have a forward propulsion phase (push-off). Therefore, some findings may vary slightly if participants were required to generate a forward impulse. Second, we have only reported changes in quasi-stiffness in the sagittal plane. It is possible that other concomitant changes may have occurred in the frontal or transverse planes (Maharaj et al., 2016, 2017). Finally, we are limited to generic, multi-segment foot models, resulting in modelling a number of small joints as one individual joint. While this method provides good general insight into how the foot functions independently of the ankle, the results found here could be strengthened via the use of biplanar videoradiography, wherein the direct motion of the talus could be measured (Kessler et al., 2019).

5. Conclusion

The outcomes from this study suggest that the midfoot can increase quasi-stiffness in a manner similar to the ankle. However, the increase in midfoot quasi-stiffness is not driven by increased intrinsic foot muscle activation during contact. The results from this study also suggest that interpretations of foot and ankle power contributions can be significantly affected by the ankle model chosen.

Acknowledgements

Declaration of Competing Interest

The authors declare that the research was conducted in the absence of any commercial or financial relationships that could be construed as a potential conflict of interest

Appendix A. Supplementary material

Supplementary data to this article can be found online at https://doi.org/10.1016/j.jbiomech.2020.109853.

References

Alexander, R.M., Bennet-Clark, H.C., 1977. Storage of elastic strain energy in muscle and other tissues. Nature 265, 114–117.

Arampatzis, A., Bruggemann, G.P., Metzler, V., 1999. The effect of speed on leg stiffness and joint kinetics in human running. J. Biomech. 32, 1349–1353.

Blickhan, R., Full, R.J., 1993. Similarity in multilegged locomotion - bouncing like a monopode. J. Comp. Physiol. A. 173, 509–517.

Bobbert, M.F., Huijing, P.A., van Ingen Schenau, G.J., 1986. An estimation of power output and work done by the human triceps surae muscle-tendon complex in jumping. J. Biomech. 19, 899–906.

Brehm, M.A., Harlaar, J., Schwartz, M., 2008. Effect of ankle-foot orthoses on walking efficiency and gait in children with cerebral palsy. J. Rehabil. Med. 40, 529–534.

Bruening, D.A., Cooney, K.M., Buczek, F.L., 2012. Analysis of a kinetic multi-segment foot model. Part I: Model repeatability and kinematic validity. Gait Posture 35, 529–534.

Cavagna, G.A., Kaneko, M., 1977. Mechanical work and efficiency in level walking and running. J. Physiol. 268, 467–481.

Domire, Z.J., Challis, J.H., 2007. The influence of squat depth on maximal vertical jump performance. J. Sports Sci. 25, 193–200.

Farley, C.T., Blickhan, R., Saito, J., Taylor, C.R., 1991a. Hopping frequency in humans - a test of how springs set stride frequency in bouncing gaits. J. Appl. Physiol. 71, 2127–2132.

Farley, C.T., Blickhan, R., Saito, J., Taylor, C.R., 1991b. Hopping frequency in humans: a test of how springs set stride frequency in bouncing gaits. J. Appl. Physiol. 1985 (71), 2127–2132.

Farley, C.T., Gonzalez, O., 1996. Leg stiffness and stride frequency in human running. J. Biomech. 29, 181–186.

Farris, D.J., Kelly, L.A., Cresswell, A.G., Lichtwark, G.A., 2019. The functional importance of human foot muscles for bipedal locomotion. Proc. Natl. Acad. Sci. USA 116, 1645–1650.

Ferris, D.P., Farley, C.T., 1997. Interaction of leg stiffness and surfaces stiffness during human hopping. J. Appl. Physiol. 82 (1985), 15–22. discussion 13-14.

Ferris, D.P., Louie, M., Farley, C.T., 1998. Running in the real world: adjusting leg stiffness for different surfaces. Proc. Biol. Sci. 265, 989–994.

Hicks, J.H., 1954. The mechanics of the foot. II. The plantar aponeurosis and the arch. J. Anat. 88, 25–30.

Kelly, L.A., Cresswell, A.G., Farris, D.J., 2018. The energetic behaviour of the human foot across a range of running speeds. Sci. Rep. 8, 10576.

Kelly, L.A., Cresswell, A.G., Racinais, S., Whiteley, R., Lichtwark, G., 2014a. Intrinsic foot muscles have the capacity to control deformation of the longitudinal arch. J. R. Soc. Interface 11, 20131188.

Kelly, L.A., Farris, D.J., Cresswell, A.G., Lichtwark, G.A., 2019. Intrinsic foot muscles contribute to elastic energy storage and return in the human foot. J. Appl. Physiol. 1985 (126), 231–238.

Kelly, L.A., Kuitunen, S., Racinais, S., Cresswell, A.G., 2012. Recruitment of the plantar intrinsic foot muscles with increasing postural demand. Clin. Biomech. (Bristol, Avon) 27, 46–51.

Kelly, L.A., Lichtwark, G., Cresswell, A.G., 2014b. Active regulation of longitudinal arch compression and recoil during walking and running. J. R. Soc. Interface 12.

Kelly, L.A., Lichtwark, G.A., Farris, D.J., Cresswell, A., 2016. Shoes alter the spring-like function of the human foot during running. J. R. Soc. Interface 13.

Ker, R.F., Bennett, M.B., Bibby, S.R., Kester, R.C., Alexander, R.M., 1987. The spring in the arch of the human foot. Nature 325, 147–149.

Kerdok, A.E., Biewener, A.A., McMahon, T.A., Weyand, P.G., Herr, H.M., 2002. Energetics and mechanics of human running on surfaces of different stiffnesses. J. Appl. Physiol. 1985 (92), 469–478.

Kessler, S.E., Rainbow, M.J., Lichtwark, G.A., Cresswell, A.G., D'Andrea, S.E., Konow, N., Kelly, L.A., 2019. A direct comparison of biplanar videoradiography and optical motion capture for foot and ankle kinematics. Front. Bioeng. Biotechnol. 7, 199.

Kura, H., Luo, Z.P., Kitaoka, H.B., An, K.N., 1997. Quantitative analysis of the intrinsic muscles of the foot. Anat Record 249, 143–151.

Latash, M.L., Zatsiorsky, V.M., 1993. Joint stiffness - myth or reality. Hum. Movement Sci. 12, 653–692.

Leardini, A., Benedetti, M.G., Berti, L., Bettinelli, D., Nativo, R., Giannini, S., 2007. Rear-foot, mid-foot and fore-foot motion during the stance phase of gait. Gait Posture 25, 453–462.

Leardini, A., Benedetti, M.G., Catani, F., Simoncini, L., Giannini, S., 1999. An anatomically based protocol for the description of foot segment kinematics during gait. Clin. Biomech. (Bristol, Avon) 14, 528–536.

Lichtwark, G.A., Wilson, A.M., 2005. In vivo mechanical properties of the human Achilles tendon during one-legged hopping. J. Exp. Biol. 208, 4715–4725.

Maharaj, J.N., Cresswell, A.G., Lichtwark, G.A., 2016. The mechanical function of the tibialis posterior muscle and its tendon during locomotion. J. Biomech. 49, 3238–3243.

Maharaj, J.N., Cresswell, A.G., Lichtwark, G.A., 2017. Foot structure is significantly associated to subtalar joint kinetics and mechanical energetics. Gait Posture 58, 159–165.

McMahon, T.A., Cheng, G.C., 1990. The mechanics of running: how does stiffness couple with speed?. J. Biomech. 23 (Suppl 1), 65–78.

Moir, G.L., 2008. Three different methods of calculating vertical jump height from force platform data in men and women. Meas. Phys. Educ. Exerc. 12, 207–218.

Muller, R., Siebert, T., Blickhan, R., 2012. Muscle preactivation control: simulation of ankle joint adjustments at touchdown during running on uneven ground. J. Appl. Biomech. 28, 718–725.

Riddick, R., Farris, D.J., Kelly, L.A., 2019. The foot is more than a spring: human foot muscles perform work to adapt to the energetic requirements of locomotion. J. R. Soc. Interface 16, 20180680.

Rouhani, H., Favre, J., Crevoisier, X., Aminian, K., 2011. Ambulatory measurement of ankle kinetics for clinical applications. J. Biomech. 44, 2712–2718.

Stearne, S.M., McDonald, K.A., Alderson, J.A., North, I., Oxnard, C.E., Rubenson, J., 2016. The foot's arch and the energetics of human locomotion. Sci. Rep. 6, 19403.

Tabachnick, B.G., Fidell, L.S., 2001. Using Multivariate Statistics. Allyn and Bacon, Boston, MA.

Thompson, B., 2006. Foundations of Behavioral Statistics: An Insight-Based Approach. Guilford Publications, New York, NY, US.

Uchida, T.K., Hicks, J.L., Dembia, C.L., Delp, S.L., 2016a. Stretching your energetic budget: how tendon compliance affects the metabolic cost of running. PLoS ONE 11.

Uchida, T.K., Seth, A., Pouya, S., Dembia, C.L., Hicks, J.L., Delp, S.L., 2016b. Simulating ideal assistive devices to reduce the metabolic cost of running. PLoS ONE 11.

Welte, L., Kelly, L.A., Lichtwark, G.A., Rainbow, M.J., 2018. Influence of the windlass mechanism on arch-spring mechanics during dynamic foot arch deformation. J. R. Soc. Interface 15.

Wu, G., Cavanagh, P.R., 1995. ISB recommendations for standardization in the reporting of kinematic data. J. Biomech. 28, 1257–1261.

Zelik, K.E., Honert, E.C., 2018. Ankle and foot power in gait analysis: Implications for science, technology and clinical assessment. J. Biomech. 75, 1–12.

Zhou, T., Zatsiorsky, V.M., Latash, M.L., 2015. Unintentional changes in the apparent stiffness of the multi-joint limb. Exp. Brain Res. 233, 2989–3004.